Journal of Applied Fluid Mechanics, Vol. 10, No. 5, pp. 1343-1353, 2017.
Available online at www.jafmonline.net, ISSN 1735-3572, EISSN 1735-3645.
DOI: 10.18869/acadpub.jafm.73.242.27582

Aerodynamic Design and Performance Assessment of a Centripetal-Flow Fan

Y. Song[1], X. Sun[1], D. Huang[1†] and Z. Zheng[2]

[1] *School of Energy and Power Engineering, University of Shanghai for Science and Technology, Shanghai 200093, China.*
[2] *Aerospace Engineering Department, University of Kansas, Lawrence, Kansas 66045-7621, USA*

†*Corresponding Author Email: dghuang@usst.edu.cn*

(Received January 1, 2017; accepted April 15, 2017)

ABSTRACT

In this paper, the aerodynamic and mechanical design of a centripetal-flow fan has been undertaken at a particular thermal environment in which the working fluid behaves as an ideal gas. A preliminary design (one-dimensional analysis) study was conducted at first, based on which three-dimensional modeling and optimization were subsequently applied to the design of the centripetal-flow fan. The aerodynamic performance of the designed fan and its operating characteristics in different working conditions were assessed by means of numerical simulations. Our results suggest that isentropic efficiency and pressure ratio of the centripetal-flow fan at design operating conditions can reach 81.14% and 1.0833, respectively, which satisfy the requirements for fans in commercial and industrial applications. From the fan performance curves, it is found that as the mass flow rate increases, the efficiency of the fan operating at the designed rotational speed first increases and then decreases. There exists an optimal mass flow rate which leads to the maximum efficiency of the fan. Similarly, the fan pressure ratio first increases as the mass flow rate increases, attains a maximum value and then decreases as the mass flow rate further increases. At off-design rotational speeds, although the fan characteristic curves show the same tendency as those observed at the design condition. Moreover, the fan characteristic curve becomes steeper with an increased rotational speed, which means that the variations of isentropic efficiency and pressure ratio with change in mass flow rate become much greater. The results of our present study confirm the feasibility of using the centripetal-flow fan for various industrial applications.

Keywords: Centripetal-flow fan; Design performance characteristics; Numerical simulation; Feasibility.

NOMENCLATURE

c	absolute velocity	u	circular velocity
D	diameter	W	power
G	mass flow rate	w	relative velocity
H	blade height		
h	enthalpy	β	blade angle relative to the tangential direction
n	rotation speed	γ	turning angle in the rotor
P	pressure	ε	total pressure ratio
q	relative mass flow rate	η	total isentropic efficiency
r_l	leading edge radius	θ	blade thickness
r_t	trailing edge radius	ρ	density
T	temperature		

1. INTRODUCTION

Fan is a rotary machine which propels air continuously and usually consists of a rotating arrangement of vanes or blades which act on the fluid. As a result, the total energy content of the air can be increased by the mechanical action of the rotating blades. Fans have wide application in power metallurgy, petroleum, chemical engineering, spinning, mining industry and other industries. It is estimated that the total amount of electrical power

consumed by all the fans in China has accounted for about 10% of China's industrial energy consumption and thus played an important role in energy supply and demand in China. Undoubtedly the development of efficient and energy-saving fan is of great significance in saving energy, improving the nation's economy and protecting environment.

Nowadays, there are two general classifications of fans: the axial flow fan and the centrifugal fan. As they are sturdy, quiet, reliable and capable of operating over a wide range of conditions, centrifugal fans are by far the most prevalent type of fan used in a variety of different industrial applications. The flow in a centrifugal fan is subjected centrifugal force which compresses the flow giving it additional static pressure. Therefore, centrifugal fans are capable of generating higher pressure than axial fans. However, the air flows in a radial-outward direction relative to the shaft in a centrifugal fan. The specific volume of fluid would continuously keep decreasing along the flow direction. As the cross section of the fan constantly increases, the height of the blade has to be gradually reduced and as a result, the gas flow rate through the fan cannot be too large in operation. Due to mismatches between its geometrical structure and the flow characteristics inside the fan, the centrifugal fans thus have an inherent limitation. By contrast, there are few studies that have been focused on the centripetal fan. According to the published literature, the original concept of centripetal fan was first patented by Crowe (1927). Moreover, Pavlecka (1957, 1960, 1962) described the concepts of multistage centripetal compressor with supersonic and subsonic rotors by three patents and put forward the rotor blade shape profile. In addition, Shan *et al.* (2012) theoretically analyzed the aerodynamic performance of a centripetal compressor and his results predicted the feasibility of the centripetal compressor from the point of view of the energy conversion. To date, there is thus a lack of studies systematically investigating aerodynamic design process, design parameter optimization, aerodynamic performance, and off-design performance characteristics of a centripetal fan.

Based on previous studies, a centripetal -flow fan was recently designed by our research team Huang *et al.* (2015), its geometric structure is demonstrated in Fig. 1. After the gas has passed through the inlet port, it enters the rotor radially from the outside and rotational kinetic energy is converted into pressure energy of the moving fluid. The kinetic energy is further converted into pressure energy in the fan stator which also induces gas into the fan outlet radially. The advantages of this design are: the specific volume of gas gradually reduces which is compatible with a continuous reduction in cross-section of fan. The blade height varies slowly in flow direction and thus can be designed to maintain a constant height. The flow velocity and flow angle don't change along with the blade height. Therefore, the effect of variation in flow characteristics along blade height can be ignored for fan performance and force analysis. In the meantime, complexity of design and manufacturing can be greatly reduced. Meanwhile, the mass flow of fan could be adjusted by varying the blade height. So this design can be used in low pressure ratio and large volume flow fan, for instance, metro fan.

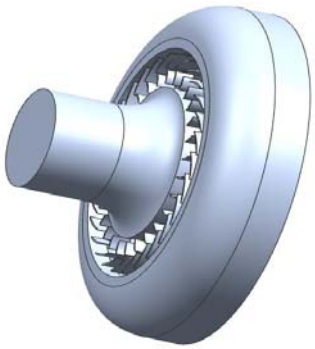

Fig. 1. The schematic of centripetal fan.

The centripetal-flow fan can be severed as a novel compress device. The design methods provide a new fresh idea for compress organic working fluid. Compared to air, specific volume of organic working fluid varies a lot in the same pressure ratio. Fig. 2 shows the volume flow ratio of different working fluid at the same temperature (310K) and pressure ratio (2). The air volume flow ratio of inlet and outlet is 1.6, yet the volume flow ratio of four organic working fluids is about 2. So this centripetal structure could be used to design working fluid pump in the ORC system and refrigerate compressor.

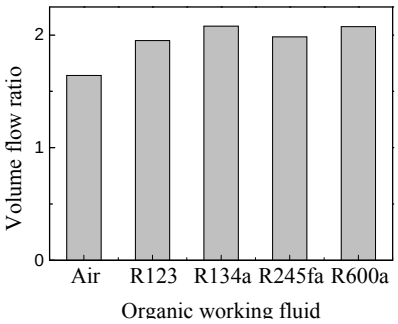

Fig. 2. Volume flow ratio with different working fluids.

In this paper, the working fluid was treated as ideal gas and then the design and off-design performance characteristics of proposed centripetal fan was assessed with the aid of computational fluid dynamics (CFD) in order to explore the feasibility of using centripetal-flow fans for various engineering applications

2. THEORETICAL AERODYNAMIC DESIGN (ONE-DIMENSIONAL ANALYSIS)

In this paper, the thermal properties of the proposed

centripetal fan were determined in advance and are presented in Table 1, which are based on technical parameters of an industrial fan.

Table 1 Centripetal fan design parameters

Parameter	Value
P_1*, Pa	101325
T_1*, K	293
P_3*, Pa	109333
ε*	1.08
G, kg/s	7.733
n, rpm	6000
η	>80%

The working fluid was treated as ideal gas for subsequent analysis conducted. A computer code has been developed to perform aerodynamic design and analysis, the key geometric parameters, efficiency and other parameters of the fan were determined based on the code analysis. Brief summaries of the main design principles applied were as follows:

1. The flow is assumed to be steady and adiabatic.
2. The inlet angle and the discharge angle are equal to 90° (gas enters and leaves both in the radial direction). The degree of reaction is set to be 1.
3. Some empirical factors for instance speed coefficient are based on both previous experience and the data adopted in Ref. written by (Aungier 2000; Bruno 1973 ; Gu et.al 2016; Song et.al 2017).

The calculation model was established referring to traditional design method of axial-flow fan in the books (Dixon and Hall 1978; Whitfield and Baines 1990). As shown in Fig. 3, subscript 1 and 2 represent the state of the working fluid at the inlet and outlet of the rotor, respectively. The flow equations can be expressed as Eq. (1):

$$\begin{cases} \text{mass continuity: } G=\rho_1 c_1 A_1=\rho_2 c_2 A_2 \sin\alpha_2 \\ \qquad\qquad \rho_1 w_1 \sin\beta_1 A_1=\rho_2 w_2 \sin\beta_2 A_2 \\ \qquad\qquad \mathrm{A}=2\pi rH \\ \text{energy equation: } h_1+\dfrac{w_1^2}{2}-\dfrac{u_1^2}{2}=h_2+\dfrac{w_2^2}{2}-\dfrac{u_2^2}{2} \\ \qquad W=\left(\dfrac{w_1^2-w_2^2}{2}+\dfrac{c_2^2-c_1^2}{2}+\dfrac{u_2^2-u_1^2}{2}\right) \\ \text{moment of momentum: } M_z=G\left(c_{2u}r_2-c_{1u}r_1\right) \\ \text{velocity triangle: } \omega_1=\sqrt{c_1^2+u_1^2-2\cdot c_1 u_1\cos\alpha_1} \\ \qquad \sin\beta_1=\dfrac{\mathrm{c}_1\sin\alpha_1}{w_1} \\ \qquad \sin\beta_2=\dfrac{\mathrm{w}_1\sin\beta_1\mathrm{r}_1\rho_1}{\mathrm{w}_2\mathrm{r}_2\rho_2} \\ \qquad \mathrm{c}_2=\sqrt{\mathrm{w}_2^2+\mathrm{u}_2^2-2\mathrm{w}_2\mathrm{u}_2\cos\beta_2} \end{cases} \quad (1)$$

Where u_1 is the peripheral speed at the inlet of the rotor, and u_2 is the peripheral speed at the outlet of the rotor, respectively. The flow enters the rotor radially from the outside, the velocity u_1 is larger than the velocity u_2, so this design is favorable to be used in low pressure ratio and large volume flow fan.

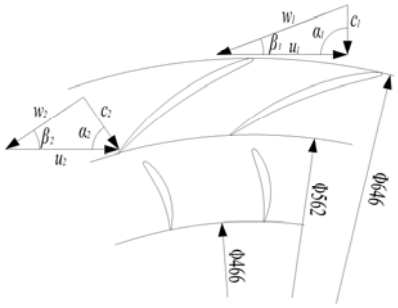

Fig. 3. Geometric plan of the elementary stage.

As a final step, the blade number were determined based on Empirical factors such as relative pitch and expelling coefficient, which are determined based on both previous experience and the data adopted in Ref. by Liu (2015). Geometric parameters including turbine rotor diameter ratio, blade height and inlet and discharge angles were optimized to ensure the best design of the centripetal fan for maximum efficiency. Table 2 summarizes the main design parameters obtained to specify the geometry of the rotor and stator.

Table 2 Centripetal fan geometry design parameters

Parameter	Value	
	rotor	stator
D_{in}, mm	646	546
D_{out}, mm	562	466
H, mm	47	47
γ, deg	15	30
Z	28	28
r_l, mm	0.75	0.75
r_t, mm	0.4	0.4

3. STRUCTURAL DESIGN OF CENTRIPETAL -FLOW FAN

3.1 Rotor and Stator Blades Geometry Design

The radius of the fan decreases along the direction of gas flows inside the fan. As a result, both the cross-sectional area of the gas flow passage and specific volume of gas decrease in the flow direction, thus forming a converging passage. The flow inside the centripetal fan exhibits substantially different physical characteristics from conventional axial fan and centrifugal fan. In this paper, an initial

blade design was conducted at first based on the aerodynamic design parameters including blade angle at inlet and outlet, blade height, inlet and outlet diameters whose values are presented in Table 2. For the purpose of brevity, only the blade profile design method for the proposed centripetal fan rotor was described in detail. As shown in Fig. 4 a two-dimensional structure on the surface of an airfoil part of the rotor blade is formed by four airfoil surface curves including the leading edge, the trailing edge, the concave surface on the pressure side of the airfoil portion and the convex surface on the suction side of the airfoil portion. A circular arc leading edge and trailing edge were used and their radiuses were 0.75mm and 0.4mm respectively, according to the blade design data for axial-flow fans in book written by Wang *et al*. (1981). The concave and convex airfoil surfaces were constructed by fixing the airfoil middle arc line at first and then adding airfoil thickness to the middle arc line Zhang and Yu (2015). As shown in Fig. 5, the middle arc line is given by a third-order Bezier curve which provides the blade angles β at various radial positions: the horizontal axis in Fig. 5 represents the radial position and the vertical axis shows the corresponding blade angle. The blade angles at the starting point and end point of the curve corresponds to the relative flow angles at inlet and outlet which are β_1 and β_4 in Fig. 5. Another two control points of the cubic Bezier curve are β_2 and β_3 whose coordinates can be varied to change the shape of the airfoil middle arc line. In addition, the airfoil thickness distribution that is superimposed to the middle arc line is also represented by one cubic Bezier curve, as shown in Fig. 6. The thicknesses at the starting point and ending point are the leading edge circle diameter θ_1 and trailing edge circle diameter θ_4, respectively. The thickness distributions at different radial positions can be obtained by changing the coordinates of another two control points θ_2 and θ_3. Finally, smooth curves described the upper and lower surfaces of the airfoil are generated to guarantee to pass through each of the control points. The similar method is also adopted to generate the stator blade shape. Fig. 7 shows the geometry of three-dimensional rotor and stator blades.

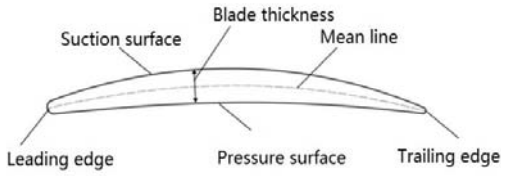

Fig. 4. 2-D model of rotor blade.

3.2 Structural Configuration Design for the Fan Inlet and Outlet Channels

In practice, external air is drawn into the fan through an inlet channel whose geometrical configuration is a curved circular duct in this work, as seen in Fig. 8. The distance of inner and outer radius of the circular duct is equal to the blade height. This design of inlet channel ensures gas enters into the fan in an axially symmetrical manner and then hits the rotor along the radial direction of the blade. As seen in Fig. 8, the bending portions of the shroud and hub surfaces are formed by using a quarter circle arc whose two ends are connected with an axially and radially extending straight portions, respectively. The geometric configuration of the outlet channel is designed by considering the structure of a centrifugal fan inlet channel (Japikse. 2000; Wang *et al*. 2013) and is illustrated in Fig. 9. Stator thus can discharge gas uniformly into the outlet channel along radial direction and the exhaust gas finally flows out the fan in the axial direction through the exit guide vane. The centerline of the outlet channel is in a shape of a quarter circle, as illustrated in Fig. 8. The hub of the fan has the form of a quarter ellipse which has the same centre as the quarter circle. A shroud is thus in the form of a truncated elliptical cone which is the surface created by the set of the quarter elliptical arcs having the same center. The cone is rounded at the top and has a top diameter of 5mm. This structural design ensures the cross-sectional area remains approximately constant across the entire outlet channel and consequently exhaust gases flowing through the channel would not change the thermal characteristics. The three-dimensional structure of the inlet and outlet channel is shown in Fig. 9.

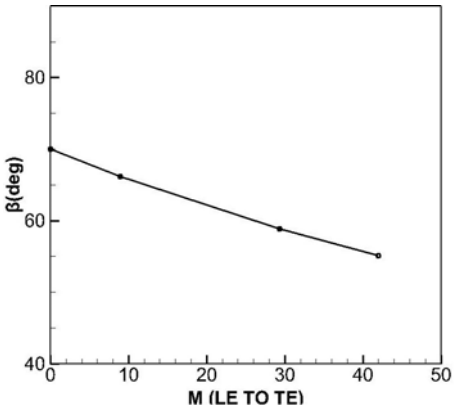

Fig. 5. Mean line angle distribution of the radial chord.

4. Two-Dimensional Simulation of a Single-Stage

A complete set of design procedures which incorporated an airfoil design for rotor and stator blades, performance prediction and airfoil shape optimization was developed with the aid of the ANSYS Workbench platform. The first step is airfoil profile design for the rotor and stator using the commercial software BladeGen. Then, the airfoil profile is inputted in ANSYS Workbench geometry module for three-dimensional modeling. In the meantime, parameters including the relative flow angles (β_2, β_3), middle-arc line thickness distribution (θ_2, θ_3) and blade number are selected for optimization in order to modify the airfoil shape

based on the flow field characteristics in the centripetal fan. Blade profile generated in BladeGen software is imported to TurboGrid module for meshing of blades and the aerodynamic performance of the designed fan in terms of the pressure ratio it generates and its efficiency is analyzed using ANSYS-CFX. The blade shape is modified repeatedly until its aerodynamic performance satisfies the design requirements.

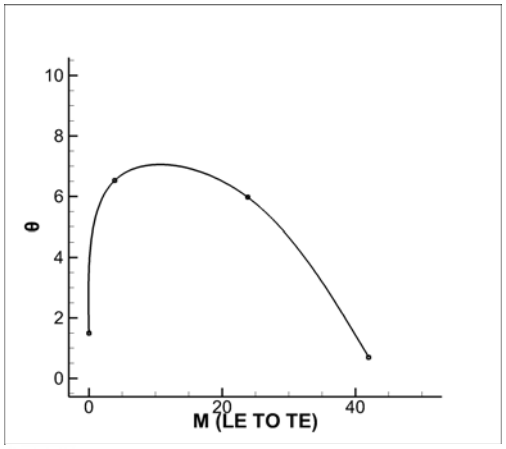

Fig. 6. Thickness distribution of the radial chord.

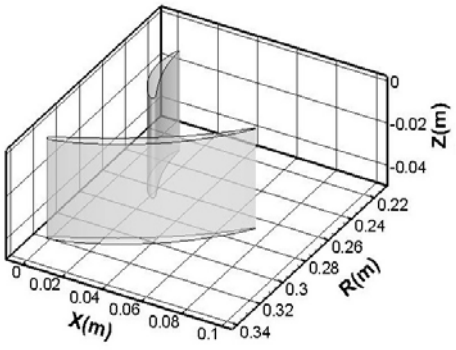

Fig. 7. 3-D model of stator and rotor blades.

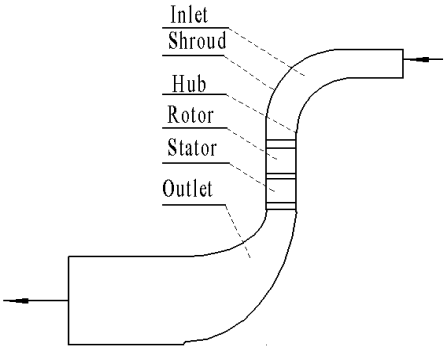

Fig. 8. Meridional view of centripetal fan.

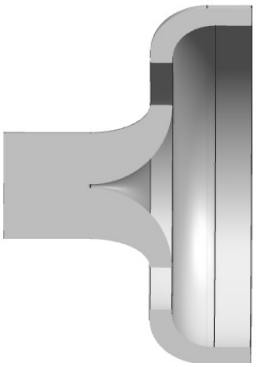

Fig. 9. 3-D model of inlet and outlet channels.

4.1 Numerical Grid Generation

A single stage centripetal fan will consist of one rotor row and one stator row. Due to the unsteady characteristics of rotor-stator interference, simulation of one blade passage is performed, reducing drastically the mesh size. In order to reduce boundary effects on the results, the inlet boundary is located 0.75c upstream from the leading edge of the rotor blade and the outlet boundary is placed 0.75c downstream of the trailing edge of the stator blade.

The computational mesh generated by TurboGrid as shown in Fig. 10. Subsequently, a grid independence study is conducted to ensure that numerical solution is independent on the grid size. A series of grids of various resolutions are thus created by changing the global size factor of mesh. The results obtained using different mesh sizes are presented in Table 3. It is found that once the total number of grid cells is greater than 51×10^4, the variations in the efficiency and total pressure ratio obtained from the simulations is less than 0.3%, and therefore a grid-independent solution has been obtained. For accuracy and cost considerations, the final mesh size used for computation then consists of 519650 elements. In addition, the mesh size used for the rotor and stator simulation is also served as a reference from which to generate the computational mesh for the complete fan configuration.

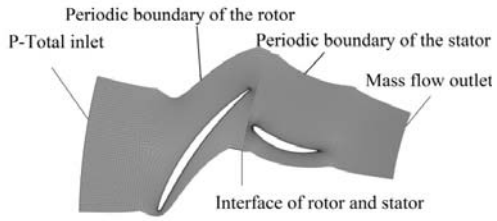

Fig. 10. Computational domain and boundary conditions for the simulation of stage.

Table 3 Grid independence check

Grid number	η , %	ε
95999	78.52	1.07298
218610	81.33	1.08229
377454	82.29	1.08456
519650	82.57	1.08546
1254620	82.8	1.0862

4.2 Defining Boundary Conditions

Figure 10 shows the computational domain and boundary conditions adopted. Total pressure and total temperature inlet boundary conditions are applied and the flow direction is normal to the boundary. Mass flow rate is specified at the outlet as boundary conditions. A no-slip wall boundary condition is used on the solid walls. The treatment used for rotor-stator interferential surface is mixing-plane method. Standard two-equation k-ε turbulent model with scalable wall wall function is applied to model the turbulent and moderate turbulence conditions (intensity=5%) intensity are considered in this study.

4.3 Numerical Results and Analysis

Table 4 reports the overall aerodynamic performance of a centripetal fan blade cascade. The total pressure ratio at the outlet is 1.08546, and the isentropic efficiency is 82.57% which exceeds the efficiency of design. As can be seen, the numerical results in Table 4 show that the rotor flow turning angle is approximately 14°, the inlet flow angle of rotor is 90° and the outlet flow angle of a stator is 89.7°. Therefore, the gas enters and leaves the stage in the almost radial direction. These numerical results suggest that the procedure described above can produce a radial fan stage that has satisfied the design requirements.

One of the major distinctions between the centripetal fan and the axial-flow fan or centrifugal fan is that the rotor and stator blades of a radial fan are straight and have the same height. As a result, there is no significant variation in flow condition along the spanwise direction of the blade and the flow can be regarded as two-dimensional. In subsequent analysis, flow characteristics at blade passage are investigated using the numerical results obtained at 50% of the blade height. As shown in Fig. 11, it is found that the flow within the blade passage is very smooth and following the curvature of the blade in stream-wise direction. No flow separation is observed to take place and block the passage between the neighboring fan blades. Fig. 12 shows the contour of eddy viscosity. It is found that there exists the wake flow behind the trailing edge of the rotor and stator blade which may result in uneven flow distribution. In addition, eddy viscosity increases only on the suction side at the exit of the rotor blade. Fig. 13 displays the Mach number contour computed in the simulated blade passage and the Mach number is subsonic. The relative velocities of flow through the rotor blade passage gradually decreases but however the absolute velocities increase. Therefore, the kinetic energy of the flow is also increased. On the other hand, as the reaction degree equals to 1, the flow velocities in a single stator blade passage remain almost constant. Static pressure contours across the blade passage are present in Fig. 14. As can be seen, the static pressure greatly increases in the rotor blade while the stator static pressure distribution nearly stays unchanged. This result suggests that the energy conversion, that is, the mechanical energy is converted into kinetic energy and pressure energy of the flow, is mainly completely by the rotor blades. These numerical results show that the centripetal fan blade model designed in this work exhibits favorable aerodynamic properties and thus is reasonable. The efficiency and pressure ratio obtained have met performance predictions. In the next step, the aerodynamic performance of a completed centripetal fan is then investigated based on the model of rotor and stator blade cascade produced in this section.

Table 4 Numerical simulation results of the centripetal fan

Parameter	Value
G, kg/s	7.73
W, kW	66.56
η ,%	82.57
ε*	1.08546
γ, deg	14

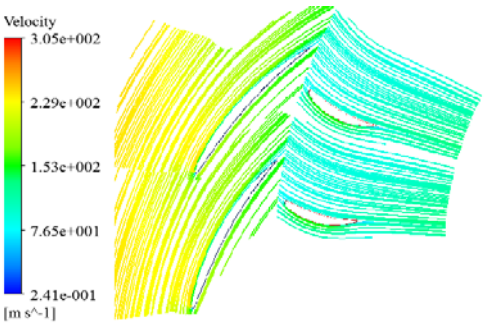

Fig. 11. Streamline distribution at 50% span.

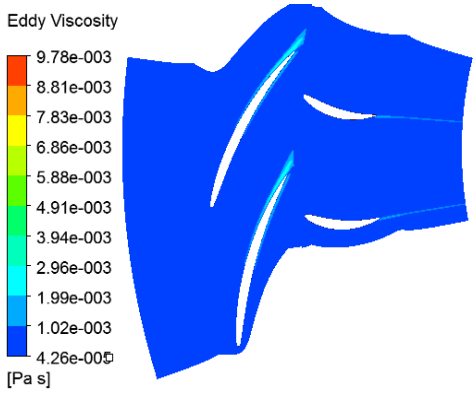

Fig. 12. Eddy viscosity distribution at 50% span.

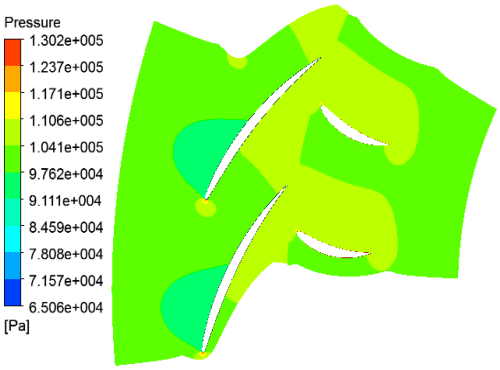

Fig. 14. The contour of static pressure distribution at 50% span.

5. NUMERICAL SIMULATION OF A CENTRIPETAL-FLOW FAN

5.1 Numerical Grid Generation

Numerical simulation of steady three-dimensional flows in a complete centripetal fan is performed with ANSYS CFX. Considering the geometric characteristics of the flow passage of a fan, a complete centripetal-flow fan proposed in this study is made up of four essential parts including inlet channel, outlet channel, rotor and stator. The structured mesh that is generated in TurboGrid is used for the rotor and stator. The meshes of the inlet and outlet channels of the 3D computational domain are created in ICEM and unstructured meshes are applied. In addition, the meshes around the places where error could be too large are locally refined to capture the physics of the problem. The computational mesh used for the simulation is illustrated in Fig. 15. A grid independence check is also performed at first. Four different sizes of grids (1.6, 3.21, 4.27 and 5.33 million cells) have been used to ensure the grid independence of the calculated results. The results provided in Table 5 suggest the mesh with 4.27 million cells for the whole computational flow domain is fine enough to achieve a mesh independent solution, and the solution doesn't change significantly upon further mesh finement.

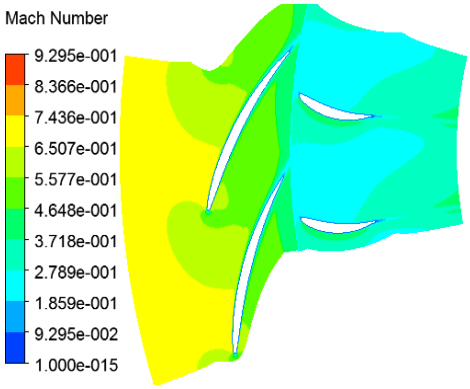

Fig. 13. The contour of Mach number distribution at 50% span.

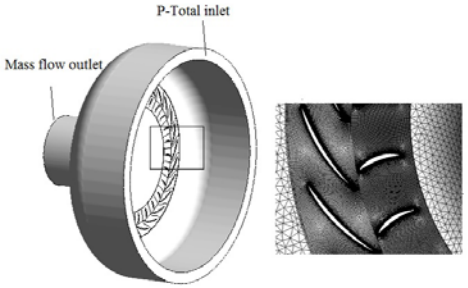

Fig. 15. Calculation model of the centripetal fan and detail of mesh.

Table 5 Grid independent verification of the centripetal-flow fan

Grid number	η , %	ε
1604950	79.5	1.08431
3215817	80.44	1.0842
4275166	81.14	1.083396
5334049	81.12	1.08336

5.2 Defining Boundary Conditions

At the inlet to the computational domain total pressure and total temperature are set. Mass flow rate is specified as boundary condition at the outlet. The fan rotation speed is set to be 6000 rpm. A no-slip boundary condition is applied at all the solid walls. The mixing-plane method is used to model the rotor-stator interface, the interface between the inlet channel and rotor and the interface between the stator and outlet channel. Separate periodic conditions are used for the rotor and stator regions. For the closure of the governing equations, the two-equation k–ε of turbulence is applied with scalable wall wall functions. The turbulence intensity used for the numerical simulation is kept constant at an intermediate level (intensity=5%).

5.3 Numerical Results and Analysis

The aerodynamic efficiency and pressure ratio calculated are summarized in Table 6. The total pressure ratio is 1.0833 and the isentropic efficiency is 81.14%, both of which meet the performance

objective that are set. However, the total pressure ratio and the isentropic efficiency of the complete fan are slightly lower than those of blade cascade. It is mainly due to the uneven flow near the guide cone in the outlet, as can be illustrated in the Figs. 16-19.

Table 6 Numeric simulation results of the centripetal fan

Parameter	Value
G, kg/s	7.73
W, kW	68.976
η,%	81.14
ε*	1.0833
γ, deg	13

Iso-contours of Mach number and streamlines in the meridian plane are illustrated in Fig. 16 and Fig. 17. Inside the fan, the flow is in subsonic regime and the streamlines smoothly pass the rotor and the stator. No flow separation or blockage occurs. However, the flow velocity distribution inside the inlet and outlet channels is not completely uniform. The region with lower speed occurs on the inlet and outlet channel elbows' outer radius. Moreover, a large central region with relatively low flow velocity appears within the flow passage of the fan. The existence of these phenomena indicates that the flow guiding cone that is formed into an elliptic shape is not properly designed and thus the flow is not uniformly distributed.

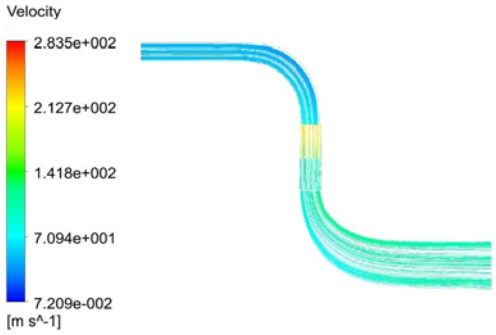

Fig. 16. Streamline distribution.

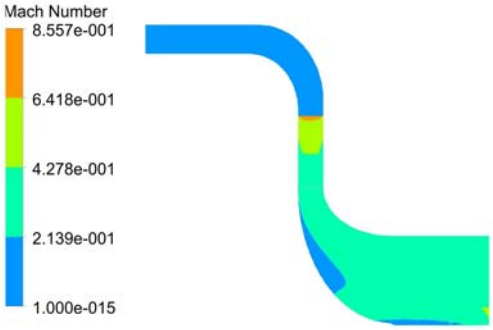

Fig. 17. Mach number contour.

Static pressure contours of the meridian surface in Fig. 18 show that the static pressure distribution along the inlet channel is uniform and the stage static pressure increases. In addition, low pressure areas at the outlet channel elbow and the central flow passage of the inlet channel are identified. Fig. 19 shows time-averaged entropy distribution through the computational domain. It can be seen that the entropy inside the centripetal-flow fan is low, suggesting that the flow losses are small in most areas of the fan. However, the large flow losses generates at the area near deflection cone at the shroud where entropy becomes abruptly greater, as shown in Fig. 19.

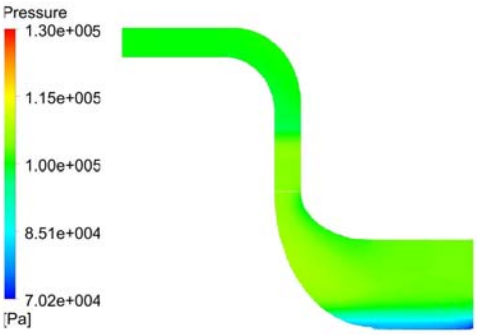

Fig. 18. Static pressure contour.

These numerical results demonstrate that the geometric design of inlet channel and rotor and stator stage is reasonable as a smooth flow pattern with no flow separation is revealed in these regions. As a result, the efficiency and total pressure ratio of the designed centripetal-flow fan are encouraging and satisfy the design requirements. Nevertheless, the configuration design of the outlet channel especially the design of the flow guide cone is still not properly and need to be optimized to reduce the flow losses and further improve the efficiency of the fan.

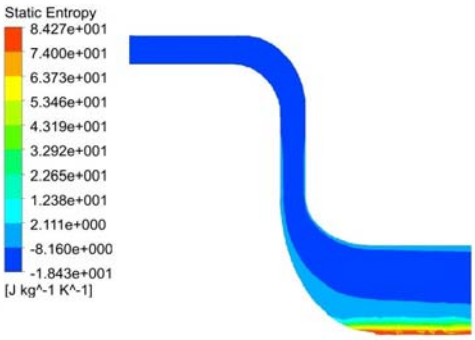

Fig. 19. Entropy contour.

6. OFF-DESIGN CHARACTERISTIC OF THE CENTRIPETAL-FLOW FAN

In practice, the centripetal-flow fans may not always operate exactly at their design conditions

and more commonly have to perform at off-design conditions (e.g. booting, halt or partial payload and so on). Therefore, it is important to study the off-design characteristics of the proposed centripetal-flow fan in an attempt to more fully grasp its operation condition. The basic parameters that can be used to describe the fan characteristic curve are total pressure ratio ε, isentropic efficiency η, mass flow rate ratio q and rotation speed n. Based on the method adopted in the study of the characteristics of a axial-flow fan (Gao *et al*. 2004;) the relative flow rate q which is defined as Eq. (2):

$$q = \frac{\frac{G\sqrt{T_1^*}}{p_1^*}}{\frac{G\sqrt{T_{10}^*}}{p_{10}^*}} \tag{2}$$

It is used as an independent variable while the total pressure ratio ε and total isentropic efficiency η are dependent variables in this paper. In this way, the performance curve drawn for the centripetal-flow fan can more directly reflect its overall performance.

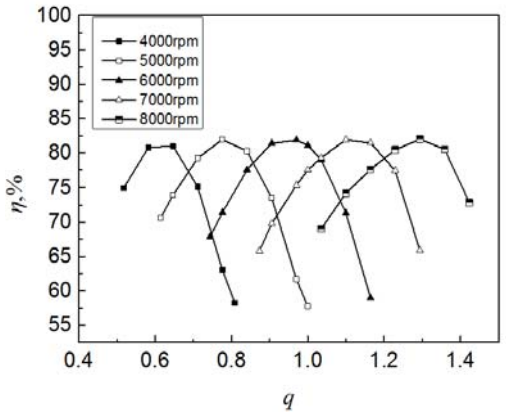

Fig. 20. Efficiency of vs. relative mass flow rate.

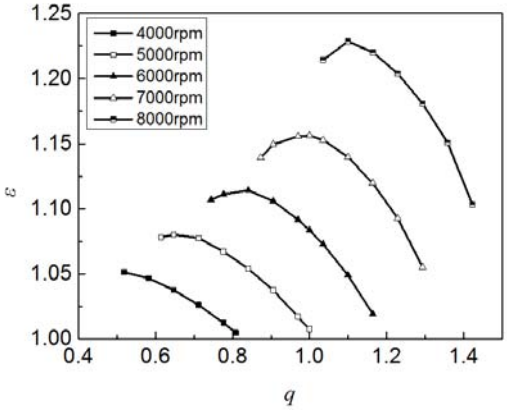

Fig. 21. Total pressure ratio of vs. relative mass flow rate.

The performance curve in Fig. 20 presents the variation of total isentropic efficiency η of the fan with relative mass flow rate q. Fig. 21 shows the total pressure ratio ε curve plotted in function of the relative mass flow rate q. It is found that the performance characteristics of the studied centripetal-flow fan have some similarity to the axial-flow fan and have been summarized into the following three points:

1. At the fan's design point rotational speed, the total pressure ratio increases first with relative mass flow rate, reaches a maximum then decreases later if the inlet total pressure and total temperature are constrained to be constant. Hence, there exists an optimal value of q. The η vs. q plot shows a similar tendency and there is also an optimal q value to achieve the highest efficiency. When q is smaller than its optimal value, the efficiency will decrease because of the decreasing flow rate. Once the value of q decreases to a certain level, fan stall occurs and the fan reaches its stable operating range limit. The corresponding q is known as critical flow rate. On the other hand, when the value of q is larger than its optimal value, the efficiency will also decrease with increasing q due to large flow losses. Beyond a certain value, an increase in q will lead to choking. The mass flow rate at choked condition is the maximum mass flow rate of the fan.

2. In this paper, the off-design characteristic curves for a centripetal-flow fan are also examined using five different rotational speeds of 4000 rpm, 5000 rpm, 6000 rpm, 7000 rpm and 8000 rpm, as illustrated in Figs 20 and 21. The numerical results suggest that all the curves behave in similar way as those obtained at design condition. There are optimal mass flow rates at different rotational speed to obtain the maximum efficiency and total pressure ratio. In addition, the characteristic curves at different rotational speed have slightly different shape: the speed is increasing while the curve becomes steeper. This suggests that the variation of efficiency and total pressure ratio with mass flow rate becomes more intense on increasing the rotational speed. It is worth noting that a large deviation from the fan's performance at design condition is found at the low rotational speed of 4000 rpm. As shown in Fig. 21, the maximum pressure ratio at 4000 rpm occurs at surge point and thus the ε-q curve obtained at the rotational speed of 4000 rpm has a general continuous declining trend.

3. The maximum values of efficiency at different rotational speeds are close to each other while the optimal value of mass flow rate to achieve the maximum efficiency becomes greater with increasing rotational speed. The maximum value of total pressure ratio increases along with the increase in rotational speed. In addition, the value of critical mass flow rate, at which surge and choking will occur, also increases with the increase in the rotational speed of the simulated fan.

7. CONCLUSION

A novel centripetal-flow fan that uses ideal gas as working fluid was designed. The adopted design method and the fan's performance characteristics are described in this paper. ANSYS CFX and related software which are CFD tools are used for design and numerical analysis. Based on the numerical results presented, the following conclusions can be drawn:

1. The results obtained from one-dimensional aerodynamic design and CFD calculations show that the total isentropic efficiency of a centripetal-flow fan can reach more than 80% and the total pressure ratio at the design condition satisfies the design requirements. Therefore, the concept of centripetal-flow fans is promising and can be used for various engineering applications.
2. The overall aerodynamic performance of fan was assessed. It is found that the flow within the blade passage is very smooth. No flow separation is observed to take place and block the passage between the neighboring fan blades. However, the total pressure ratio and the isentropic efficiency of fan are slightly lower than those of blade cascade. It is mainly because that the elliptic shape flow guiding cone is not properly designed form and thus the flow is not uniformly distributed. The outlet channel would be optimized to reduce the flow losses and further improve the efficiency of the fan.
3. The performance characteristics of the proposed centripetal flow fan at off-design conditions were examined using numerical simulation method. The present results show that both the total isentropic efficiency and total pressure ratio of the centripetal-flow fan increase as the mass flow rate increases at first, reaches the maximum value and then decreases. Thus, there are different optimal values for the mass flow rate to achieve the maximum efficiency and total pressure ratio, respectively. Compared with the performance curves obtained at design condition, the variation of efficiency and total pressure ratio with mass flow rate becomes more severe on increasing the rotational speed of fan. The performance curves at off-design conditions become steeper at higher rotational speed.
4. Compared to the conventional axial-flow fans and centrifugal fans, the centripetal-flow fan has the advantage that its structural design is highly compliant with the aerodynamic flow field behavior inside the fan. The blades of a centripetal-flow fan can be designed to have the same height as the flow field doesn't change much in general along the blade height. As a result, the blade manufacturing process becomes more convenient and efficient. Furthermore, the centripetal-flow fan can also operate at high flow rate condition.
5. The centripetal-flow fan can be severed as a novel compressor. The design methods presented in this study thus provide a new fresh idea for refrigeration compressors that use organic working fluid with specific thermodynamic properties such as high molecular weight and a large specific volume change.

ACKNOWLEDGEMENTS

This work was supported by National Natural Science Foundation of China (Grant Nos. 51536006 and 91530111).

REFERENCES

Aungier, R. H. (2000). Centrifugal compressors: a strategy for aerodynamic design and analysis. ASME Press, New Yoke, U.S.

Bruno Ec, k. (1973). Fans: design and operation of centrifugal, Axial-Flow and cross-Flow Fans. Pergamon Press LTD, London, England.

Crowe, P. L. (1927). Patent, Centripetal compressor. Docket No.1644565, U.S.

Dixon, S. L. and C. A. Hall (1978). Fluid mechanics and thermodynamics of turbomachinery, Pergamon Press Ltd 20-50.

Gao, X. L., Z. R. Lin and X. Yuan (2004). Calculation of the overall aerodynamic performance of multi-Stage axial-Flow compressor. *Thermal Turbine 33(3)*, 195-199.

Huang, D. G., Y. G. Li and X. Tan (2015). Patent, The radial compressor. Docket.

Japikse. D. (2000). Turbomachinery diffuser design technology. Concepts ETI Inc, White River Junction, U.S.

Liu, S. S. and H. MA (2015). Parameterization of modeling the areo-turbine balde based on CATIA. *Ordnance Industry Automation 34(4)*, 56-63.

Pavlecka, V. H. (1957). Patent, Gas turbine power plant with a supersonic centripetal flow compressor and a centrifugal flow turbine. Docket.

Pavlecka, V. H. (1960) Patent, Supersonic centripetal compressor. Docket.

Pavlecka, V. H. (1962). Patent, Methods of compressing fluids with centripetal compressors. Docket.

Shan, P. and J. Y. Wang (2012) The feasibility study of centripetal compressor. *Academy of Engineering Thermophysics and the Annual Conference of Engine Aerothermodynamics Academic*.

Song, J., C. W. Gu and X. S. Li (2017). Performance estimation of Tesla turbine applied in small scale Organic Rankine Cycle (ORC) system. *Applied Thermal Engineering*

110, 318–326.

Wang, Y., K. Wang, Z. Tong and *et al*.(2013). Design and optimization of a single stage centrifugal compressor for a solar dish-brayton system[J]. *Journal of Thermal Science 22(5)*,404-412.

Wang, Z. Q. and R. Qin (1981). Turbomachinery principle machine. CMP, Beijing.

Whitfield, A. and N. C. Baines (1990). Design of radial turbomachines. ESSEX, England.

Zhang, X. D. and S. M. Yu (2015). Modeling and optimization for turbine blades based on bezier curve. *Journal of Mechanical Strength 37(2)*, 266-271.